Thermal and Spectroscopic Characterization of Thermally Induced Transitions in Sequential Copolymers Containing Thioethylene Units

Jeno Muthiah and Lon J. Mathias*

Department of Polymer Science, University of Southern Mississippi, Hattiesburg, Mississippi 39406-0076

Received March 1, 1995; Revised Manuscript Received September 5, 1995[⊗]

ABSTRACT: In this paper, we describe the thermal and spectroscopic analysis of copolymers containing sequential thioethylene units. Room-temperature analysis of copolymers confirms structures similar to poly(thioethylene) (PTE) for the thioethylene segment in copolymers with oxyethylene spacers. With poly(methylene) spacers, the overall conformation along the polymer chain is different from that of PTE, leading to different crystal packing and reduced melting points. DSC shows multiple transitions for the oxyethylene copolymers. Variable-temperature spectroscopic analysis indicates a nonconcerted conformational disorder in the *rigid* regions of the oxyethylene copolymers at temperatures well below both DSC submelting and melting transition temperatures. Reorganization involving crystal thickening may be occurring at intermediate DSC exotherms seen just before the final melting endotherm. Conformational disorder occurs sooner and to a greater extent in sequential copolymers in which the spacer group consists of poly(methylene) units rather than oxyethylene between thioethylene segments, and there is reduction or absence of the premelt transitions in many of these samples.

Introduction

Oxyethylene and thioethylene polymers and oligomers appear structurally similar, yet possess vastly different chemical and physical properties. Poly(oxyethylene) (POE) is water and organic soluble,[1] crystallizes in a 7_2 helix, and melts at ca. 68 °C.[2] Poly(thioethylene) (PTE) is insoluble in virtually all solvents, crystallizes in a 2_1 helix (or glide plane), and melts at over 200 °C.[3-5] The ether groups of linear and cyclic oxyethylene oligomers complex readily with alkali metal salts, but interact weakly with transition metal ions.[6] Thioether compounds interact strongly with transition metal ions, but weakly with alkali ions.[7] The physical and chemical differences between these two families of materials are directly related to carbon–heteroatom bond lengths and angles,[8] outer shell orbital availability, electron pair configuration, and relative hardness or softness.

We have been studying copolymers of thioethylene and oxyethylene possessing sequential repeat units to synthetically evaluate whether synergistic or averaged properties derive from the number and distribution of moieties along the polymer chain. We and others have previously reported the synthesis of sequential copolymers that, on heating, showed, unusual DSC thermal behavior with two endotherms on either side of an exotherm.[9-13] This behavior is very similar to that of poly(butylene terephthalate) (PBT), which shows melting–recrystallization–remelting phenomena associated with the existence of a thermodynamically stable high-temperature crystal form.[14] Direct crystal–crystal transformations can lead to multiple peaks (two endotherms, no exotherm) on heating and single exotherms on cooling, as seen for polyamides in general[15] and nylon 11 specifically[16] in which different crystal forms (α and δ) are stable at different temperatures.

In the preceding paper in this issue, we examined a series of model compounds of structure $CH_3(CH_2)_9$–$S(CH_2CH_2S)_n$–$(CH_2)_9CH_3$ to understand the molecular level (conformational) behavior associated with multiple DSC transitions. Conformational motion at the C–S bonds of the thioethylene segment was demonstrated to occur, involving gradual initial conversion of gauche to trans isomers that eventually resulted in concerted solid–solid transitions in some samples. This gauche-to-trans conversion was shown to begin at a much lower temperature than the DSC transition observed first and is characterized in solid state ^{13}C NMR by the reduction of γ-gauche shielding and the introduction of β-sulfur shielding effects. This gauche-to-trans conversion was also observed by reduction of the CH_2 rocking and C–S stretching bands associated with thioethylene segments in gauche conformations in FT-IR and FT-Raman spectra, respectively. The all-trans conformation at the thioethylene segment is related to increased distance between these molecules. In samples showing solid–solid transitions observed as first-order endotherms in DSC traces, discontinuous changes are observed in ^{13}C chemical shifts, ^2H splitting constants, and the intensities and frequencies of certain IR vibration modes. All spectral data confirmed the formation of a unique crystal form stable at high temperature, with trans conformations at all C–S bonds and overall increased chain mobility. Thus, two types of thermally induced molecular processes are observed in these crystalline model compounds: nonconcerted increases in *trans*-thioether conformations, occurring gradually with increasing temperature below premelt transitions, and concerted conversion of all gauche-to-trans conformers seen as an endothermic DSC peak, which correlates with discontinuous spectral changes to confirm the conformational changes. The former involves increased librational motion with gradual expansion of the crystal lattice, and the latter involves a rapid, reversible transition between two thermodynamically stable crystal forms.

The copolymers made earlier showed that T_m was enhanced by increasing the relative number of thioethylene units in the copolymer. The copolymer with the highest melting point made previously had three thioethylene units separated by one oxyethylene unit. An additional goal of this paper was to further study the effect of the spacer group between thioethylene seg-

[⊗] Abstract published in *Advance ACS Abstracts,* November 1, 1995.

0024-9297/95/2228-7806$09.00/0

ments on polymer properties by extending the number of thioethylene groups to four and incorporating poly(methylene) segments in place of oxyethylene groups in a separate family of polymers. Key to this study is the detailed spectroscopic observation of crystal packing and segmental motion, leading to an understanding of the thermal behavior of the polymers in comparison to the oligo(thioethylene) model compounds.

Experimental Section

1,5-Dichloro-3-oxapentane (2-chloroethyl ether), sodium hydride (NaH), and the α,γ-dibromoalkanes were used as obtained from Aldrich Chemical Company. 1,4,7-Trithiaheptane (2-mercaptoethyl thioether) was obtained from Nisso Maruzen Chemical Company and distilled before use. 1,4,7,10-Tetrathiadecane (3,6-dithiaoctane-1,8-dithiol, **1**) was synthesized as reported earlier.[17] 2,5,8,11,14-Pentaoxapentadecane (tetraglyme or tetraethylene glycol dimethyl ether) was dried over molecular sieves for 48 h before use. All other solvents were used without further purification unless specified otherwise.

Thermal analysis was carried out with a Perkin-Elmer DSC 7 equipped with an IBM microcomputer. The heat capacity values were measured as areas above the base line for endotherms and below the base line for exotherms. The endotherm heat capacities are approximate due to overlying exotherms on the heating run. Solution ^{13}C NMR spectra were obtained on Bruker AC-200 and AC-300 spectrometers. All solid state spectroscopic analyses involved samples that were crystallized slowly from the melt. ^{13}C CP/MAS and HP/MAS data were obtained on a Bruker MSL-200 equipped with a Bruker solids probe. Raman measurements were made on a Bruker IFS 88 spectrometer with an FRA 106 Raman module using a laser power of 500–600 mW to avoid sample heating. High-temperature spectra were obtained using an Omega high-temperature cell, with the sample packed in glass tubes of 5 mm diameter. Temperatures were corrected for laser heating by measuring the temperature increase at room temperature upon introducing a thermocouple into the path of the laser beam at 600 mW. IR analysis was performed on a Perkin-Elmer 1600 FT-IR operating at a resolution of 2 cm^{-1}. An Omega variable-temperature unit was used for the acquisition of high-temperature IR spectra. Sample preparation involved melting the sample between two KBr IR windows and cooling back to room temperature. Samples were maintained at each temperature for 30 min before spectral collection. X-ray data were obtained on a Siemens XDP-700P using Cu Kα radiation. All measured temperatures (spectral and X-ray data) are estimated to be accurate to within ±2 °C. Nominal temperatures reported in some sections do not agree exactly, although qualitative correlation with DSC transitions and between different methods is very good.

Polymerization Procedure for 2a,b and 3a–e. Copolymers of structure $[(CH_2CH_2S)_n-CH_2CH_2O]_m$ (**2a** and **2b**, n = 3, 4) were synthesized by polycondensation of dimercaptans and 2-chloroethyl ether in tetraglyme. Synthesis of $[S(CH_2CH_2S)_2-(CH_2)_n]_m$ (**3a–e**, n = 5, 7–10) polymers was achieved by reacting dimercaptoethyl thioether with various α,γ-dibromoalkanes under similar conditions. The general synthetic scheme for copolymers is given in Figure 1. A typical procedure involved dissolving 3,6-dithiaoctane-1,8-dithiol (0.558 g, 2.47 mmol) in 10 mL of dried tetraglyme. To this was added 2-chloroethyl ether (0.354 g, 2.47 mmol) and NaH (0.24 g, 10 mmol). The reaction was stirred for 12 h at room temperature under N_2 and then poured into cold methanol and filtered. The filtrate was stirred in hot chloroform, and the solid–liquid mixture was poured into acetone. The precipitate was filtered and dried at ambient temperature under reduced pressure to yield **2b** (0.42 g, 57% yield); ^{13}C NMR (in 1,1,2,2-tetrachloroethane with DMSO-d_6 insert): δ 30.3 ($\mathbf{S}CH_2CH_2O$), 31.0 ($\mathbf{S}CH_2\mathbf{C}H_2SCH_2CH_2O$), 31.3 ($\mathbf{C}H_2SCH_2\mathbf{C}H_2SCH_2CH_2O$), 71.1 ($CH_2\mathbf{C}H_2O$). Copolymers containing poly(methylene) chains as spacers between the thioethylene segments (**3a–e**) were dissolved in hot chloroform and precipitated into cold methanol.

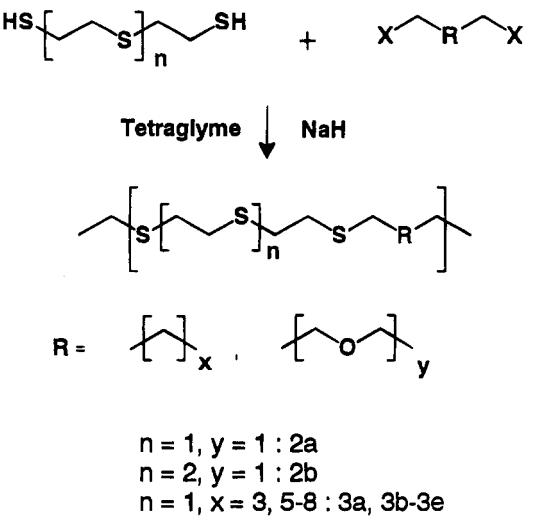

n = 1, y = 1 : 2a
n = 2, y = 1 : 2b
n = 1, x = 3, 5-8 : 3a, 3b-3e

Figure 1. General synthesis of thioethylene copolymers studied here.

Results and Discussion

General Characterization Considerations. Discussions of the DSC results in this paper deal with only the crystalline regions of the sample, as the T_g's of both homopolymers of POE and PTE are below room temperature and those of the copolymers should be as low or lower. The crystalline contents of these copolymers were estimated to be on the order of 20–40% by comparing the heat capacities of melting for the copolymers and PTE. The heat capacities for both crystallization and melting of these copolymers are in the range of 60–100 J/g, as compared to 160 J/g for PTE of ca. 55% crystallinity.[3,9]

Other methods were used to examine the samples' crystalline domains, amorphous regions, and partially ordered interphases; the interphase region is defined as one with rigidity intermediate between those of the crystalline and amorphous regions. The following methods allow specific observation of some or all of these as indicated. X-ray analysis involves only the ordered arrangement of polymer chains over extended arrays, i.e., it "sees" mainly larger crystalline domains. IR and Raman spectroscopies nonselectively probe all amorphous, crystalline, and interphase regions of a semicrystalline sample. ^{13}C CP/MAS looks at the rigid domains (both crystalline and the rigid interphase), but does not readily observe mobile amorphous regions. At higher temperatures, the contribution from the rigid interphase to ^{13}C CP/MAS spectra diminishes or disappears. ^{13}C HP/MAS, on the other hand, looks more at the mobile amorphous component of a semicrystalline sample. At high temperatures, peaks often sharpen (due to increased mobility) and increase in intensity due to added contributions from the interphase to the mobile component). The discussions in later sections involve the use of each of these techniques to examine all or part of the solid copolymer samples at ambient and elevated temperatures.

Syntheses. Synthesis of monomer **1** allowed the extension of the sequence of thioethylene units to six in the model compounds (reported in the preceding paper) and to four in the copolymer series. Initial attempts at phase transfer polycondensation between dimercaptans and dihalides did not yield copolymers of high molecular weight compared to polymers formed through the bis(isourea) intermediates.[9] This was due to the early precipitation of polymers from the benzene organic phase. The high nucleophilicity of the thiol anions prohibited the use of chlorinated solvents in

Table 1. Yields, Viscosities, and Upper Melting Points of Solution-Precipitated Copolymers

copolymer	% yield	$[\eta]$ (dL/g)	T_m^{II} (°C)
2a	53.7	0.20[a]	129
2b	57.5	0.19[a]	135
3a	65.0	0.49[b]	91
3b	71.2	0.36[c]	104
3c	88.2	0.33[c]	95
3d	45.0	0.27[c]	89
3e	71.9	0.28[c]	92

[a] In 1,1,2,2-tetrachloroethane at 60 °C. [b] Inherent viscosity at 0.4 g/dL in chloroform at 30 °C. [c] In chloroform at 30 °C.

which the polymers are soluble. The combination of tetraglyme and NaH worked reasonably well to give the yields, viscosities, and melting points for the copolymers reported in Table 1. Less than quantitative yields may be attributed to poor solubility in tetraglyme or formation of cyclic products, as described by others using phase transfer polymerization for analogous materials.[18] In general, intrinsic viscosity values of the copolymers were similar to those reported for related copolymers.[12] Introduction of poly(methylene) spacers increased the solubility of the copolymers, leading to higher viscosities for these materials.

During the course of preparing this manuscript, a new synthesis of related polymers appeared that extends the series to include additional sequences of thioethylene and oxyethylene units.[19] The procedure described involves tailoring the pH of the reaction with a suitable buffer to allow selective SH deprotonation and efficient interfacial reaction, leading to the buildup of high molecular weight products. In fact, the polymers described have the highest MWs of any in this family that we are aware of, ranging from moderate for an A_2B polymer (with an inherent viscosity of 0.33 dL/g) to A_2B_2 and AB_2 materials with respective viscosities of 1.28 and 1.55 dL/g and number-average MWs (measured by SEC) of 16 000 and 73 000, respectively. These three copolymers had melting points of 110, 82, and 38 °C, respectively. It should be pointed out that, in the convention used here, A refers to thioethylene units and B to oxyethylene groups in the overall repeat unit; e.g. A_2B_2 refers to the polymer $[(CH_2CH_2S)_2-(CH_2CH_2O)_2]_n$.

Increased solubility correlates with reduced melting points of copolymers with poly(methylene) spacers compared to copolymers with an oxyethylene unit as spacer. Copolymers **3a–e** and **2a** have similar thioethylene segment lengths (containing three thioether units) along the backbone. However, the dissimilarity in melting points between the series **3a–e** and **2a** suggests different crystalline packing. The question raised is as follows: Do the oxyethylene and poly(methylene) moieties disrupt, enhance, or have little effect on the crystalline packing and thermal behavior of the thioether segments? We attempt to answer this question by first examining the melting behavior of all sequential copolymers in the PTE–POE series that we are aware of, second, establishing the ambient-temperature crystalline properties of individual copolymers reported here, and last, evaluating motion and packing behavior with increasing temperature by using various physical and spectroscopic methods.

Melting Point Correlation with Copolymer Sequence. We previously published a preliminary correlation of melting points with sequence type and distribution for several thioethylene copolymers.[10] Litt and co-workers recently added three data points to this family,[19] and the polymers described here contribute several more. Figure 2 gives the overall plot of all of these values, with melting points related to the mole fraction of thioethylene units in the polymer repeat unit; i.e., for polymer A_mB_n, the mole fraction used here is $m/(m + n)$. This results in values of 0 and 1 for the homopolymers of POE and PTE. On the plot, two values for PTE were used (190 and 210 °C) to represent the range reported in the literature (see ref 19 for further references).

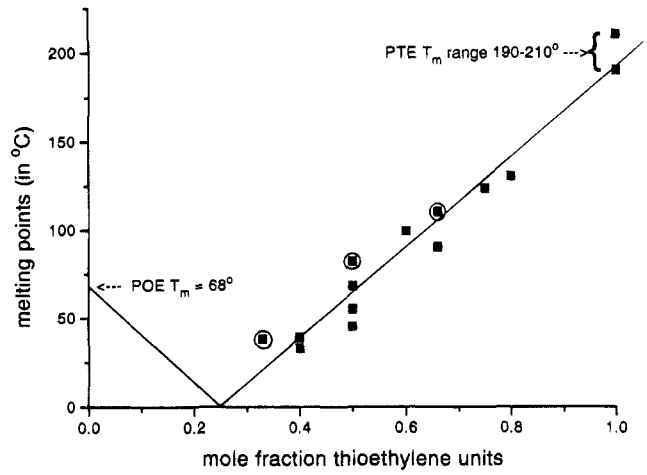

Figure 2. Plot of T_m versus mole fraction of thioethylene segments in sequential copolymers with thioethylene and oxyethylene units.

Several observations can be made about this plot. First, the circled values are from another laboratory.[19] Second, there are multiple points for mole fraction values of 0.4, 0.5, and 0.67. The first is for two copolymers with different sequences: an A_2B_2 sequence gave a melting point of 38 °C, while an $ABAB_2$ composition melted at 33 °C. Greater differences are seen for copolymers with an overall composition of 0.5, where the sequences and melting points increased in the order ABAB, 45 °C < A_2B_2, 55 °C < A_3B_3, 69 °C from our work, with a literature A_2B_2 polymer giving a higher value than ours (82 °C) because of higher MW. A similar rationale applies to two samples of A_2B copolymer, ours with a T_m of 88 °C and the literature one with T_m 110 °C.

A third observation deals with the linear least-squares analysis of this data (straight line shown in Figure 2). A correlation coefficient of 0.976 (slope 255 °C/mol fraction) was obtained using both PTE T_m values, but *not* the T_m value for POE of 68 °C. In fact, the intercept for the plot at 0 mole fraction PTE (to give an extrapolated value for POE) was −63 °C, a value that misses the actual one by ca. 130 °C. A referee has pointed out that such behavior probably results from eutectic-like lowering of the melting points of copolymers near the POE side of the plot;[20] this is illustrated by the arbitrary line drawn to connect the y-axis at the POE melting point and the least-squares fit. Unfortunately, there are no data points available for the range of copolymer compositions from 0 to 0.3 thioethylene segment mole fraction, and this line's position is purely speculative. In any event, the goodness of fit of this data to a straight line strongly suggests a real correlation between T_m and overall copolymer composition, but one that does *not* depend strongly on the actual sequence placement *in* the repeat units. This last point (as illustrated for the small range of T_m's for 0.5 mole fraction copolymers of ca. 55 °C) confirms that, for short blocks of the very different thioethylene and oxyethylene repeat units, the crystal packing represents some kind of average in terms of strength of interaction that

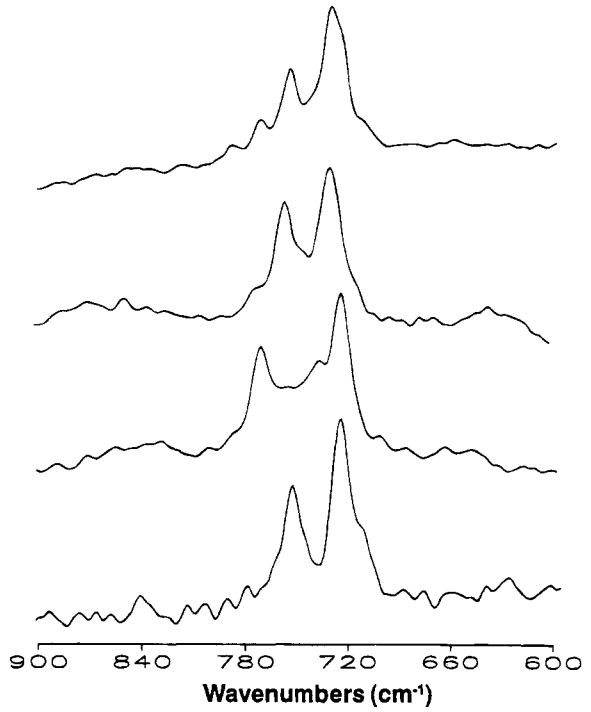

Figure 3. Room-temperature Raman spectra of solution-precipitated **2a**, **2b**, **3b**, and PTE (top to bottom).

determines the energetics of melting. We discuss this "averaging" of conformation and packing with respect to the results of molecular level spectroscopic analyses.

Ambient-Temperature Analysis of Copolymers. Room-temperature Raman analysis of copolymers should indicate the influence of poly(methylene) and oxyethylene spacers between the thioethylene segments on the coformational preferences at the thioethylene segments. The Raman spectra of **2a**, **2b**, **3b**, and PTE are given in Figure 3. It can be seen that thioethylene segments in copolymers **2a** and **2b** (top two spectra) mainly have C–S bonds in gauche conformations (giving a peak at 753 cm^{-1}), similar to PTE and the internal C–S bonds of the model compounds with longer thioethylene segments.[17] The band due to trans segments at 771 cm^{-1} appears only as a shoulder for **2a** and **2b** and is not seen in the spectrum of PTE (bottom spectrum). The trans peak may be due to segments adjacent to the oxyethylene units or those in the amorphous regions of the samples. It is weak in all three spectra despite the fact that crystalline contents are estimated to be only 20–40% (estimated from heat capacity data of cpolymers compared to that of PTE), seeming to indicate that, even in the amorphous regions, gauche conformations are preferred. Thus, the gauche conformation at the C–S bonds is preferred even for copolymer **2a**, which contains alternating sequences of three thioethylene units and a single oxyethylene moiety (see Figure 4 for the analogous conformational structure of **2b**).[21] When the C–S bond and the C–O bond are in their preferred gauche and trans conformations, respectively, then the fourth atom from oxygen (a methylene unit) is at a distance of ca. 3.78 Å. This distance can accommodate the CH_2 and the oxygen atom without steric interactions, allowing complete gauche isomer adoption by all thioethylene segments. Similar behavior explains the even higher gauch population at C–S bonds in **2b**.

In **3b**, however, the trans isomer peak for the thioether moieties is much more intense than the gauche peak (second from bottom trace in Figure 3). The ratio of the peaks at 770 (trans) and 753 cm^{-1} (gauche) is

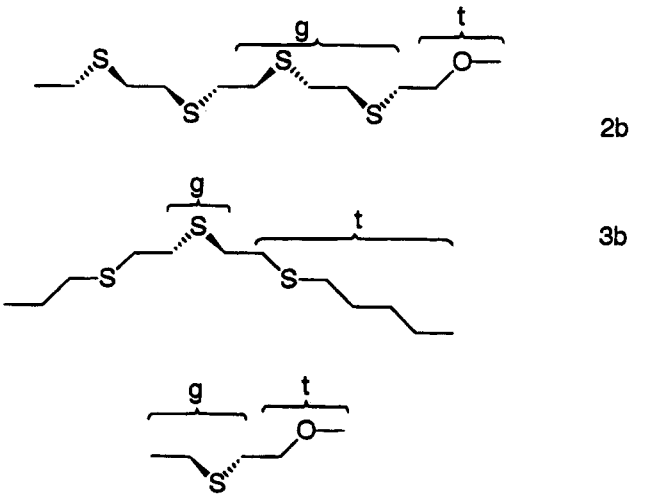

Figure 4. Conformational preferences along the polymer backbones of **2b** (top) and **3b** (middle) and in thioethylene–oxyethylene segments of poly(thiodiethylene glycol) (bottom).

approximately 2:1. The conformation along the thioethylene segment in **3b** is very similar to the decyl-capped model compound with three sulfur atoms; i.e., the C–S bonds closest to the poly(methylene) segment are forced into trans conformations, while only the internal C–S bonds adopt gauche conformations.[17] This should lead to a peak ratio of 2:1 for trans and gauche peaks of **3b**, which is consistent with what is seen in the Raman spectrum. The different effects of oxyethylene and poly(methylene) spacers on determining conformation at nearby thioethylene segments suggest that the average conformations along the backbones of the two sets of copolymers are those given in Figure 4. This difference in behavior can be explained as follows: if the oxygen atom is replaced by a methylene unit, the distance between this methylene unit and the methylene unit adjacent to sulfur and internal to the thioethylene segment (distance to the fourth atom ca. 4.0 Å) is barely enough to accommodate the van der Waals radii of the two methylene units (2.0 Å each) with the C–S in the gauche conformation. This interaction destabilizes the preferred thioether gauche conformation, resulting in the adoption of the trans conformation at the C–S bonds adjacent to poly(methylene) groups in **3b**. This effect is also seen in the model compounds where the terminal C–S bonds are in trans conformations induced by through-space interactions with the *trans*-methylenes of the decyl chains. This conformational behavior reduces intermolecular interactions between the polymer chains, resulting in lower melting points for the series of copolymers with the poly(methylene) group as spacer.

Room-temperature ^{13}C CP/MAS spectra of **2a**, **2b**, **3b**, and PTE are given in Figure 5. Most of the C–S bonds in the thioethylene segments are in the more stable gauche conformation in **2a** and **2b** (similar to PTE), as identified by the main peak at 30.8 ppm (since CP/MAS spectra enhance observation of the rigid and crystalline regions of the sample, the more intense peaks should correspond to crystalline domains). This chemical shift also matches that of the central methylene units of model compounds with longer thioethylene segments, which have their C–S bonds on both sides in gauche forms. The methylene units α and β to oxygen are seen at 71.6 and 28.0 ppm, respectively. The former is insensitive to conformation, appearing at the same chemical shift in gauche, trans, and rapidly averaging environments. The latter is, however, sensitive to the

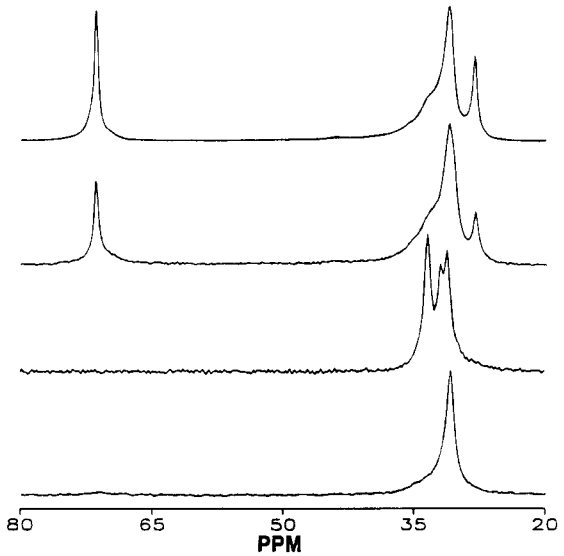

Figure 5. ^{13}C CP/MAS spectra of solution-precipitated **2a**, **2b**, **3b**, and PTE at room temperature (top to bottom).

conformation of the adjacent thioethylene group. The 28 ppm chemical shift corresponds to carbons β to oxygen, with the C−O bonds in trans conformations and thioethylene groups in the other direction in gauche conformations (see Figure 4). These chemical shift values are in good agreement with those of the carbons α and β to oxygen in *all-trans*-poly(tetramethylene oxide), and these backbone conformations are similar to those postulated for poly(thiodiethylene glycol).[21,22] The peak at 28.0 ppm is half as intense as the α-carbon peak, consistent with it representing the 30−40% of groups locked into the trans conformation around oxygen but experiencing a gauche interaction through the thioether bond; i.e., in the melt and in solution, conformational averaging with loss of most of the gauche shielding causes a large downfield shift for this peak. In the solid state spectrum, the peak for the amorphous carbons β to oxygen is shifted downfield and overlaps the broad amorphous thioether shoulder at 33.0 ppm. This was confirmed by ambient-temperature HP/MAS spectroscopy (which enhances the amorphous and mobile regions of the sample), which showed a marked increase in the intensity of the broad peak at 33.0 ppm. This shoulder was observed in the ^{13}C CP/MAS spectra of **2a** and **2b**, but was reduced in PTE due to its higher crystallinity. This assignment was further confirmed by the ^{13}C CP/MAS spectrum (not shown) of an alternating copolymer of oxyethylene and thioethylene in which a single peak corresponding to OCH_2 was seen at 71.9 ppm, while the CH_2S group was observed as two peaks at 32.8 (broad) and 28.4 ppm (sharp); the upfield resonance is due to crystalline regions and the downfield one is due to random conformations of segments in amorphous domains.

In the ^{13}C CP/MAS spectrum of **3b**, there are sharp peaks at 31.3, 31.9, and 33.3 ppm plus broad amorphous peaks under these. The peak at 33.3 ppm is due (mainly) to the central CH_2 units of the seven-carbon chain of **3b**. This poly(methylene) unit is long enough to adopt an all-trans conformation, similar to the behavior of PE and the decyl end groups of the model compounds in crystalline domains. This gives a chemical shift similar to the orthorhombic peak seen for PE. Thus, the conformational behavior of this part of the polymer is clearly confirmed by sharp peaks in the ^{13}C CP/MAS spectra and will be useful in variable-temperature studies.

On the basis of the conformational structure give in Figure 4, copolymer **3b** should have three CH_2 peaks, similar to the model compound with three sulfur atoms.[17] However, only two peaks are seen at 31.3 and 31.9 ppm, although with a higher intensity for the former. This is consistent with the 2:1 ratio of tt:tg groups expected if the tt peaks coincidentally overlap for the polymer and the 31.9 ppm tp peak is increased slightly by the broad amorphous and interphase bands underneath. The ^{13}C HP/MAS spectrum (enhanced observation of the mobile regions of the sample) showed only broad peaks at 33.0 and 29.0 ppm. The peak at 33.0 ppm is similar to that seen for the amorphous regions of **2b** and is assigned to the mobile thioethylene segments (random conformations); this peak is *downfield* from the crystalline peaks by ca. 1−2 ppm. The peak at 29.0 ppm is assigned to the alkyl groups in the amorphous regions (similar to PE) and arises from conformational averaging of the poly(methylene) units, causing an *upfield* shift of ca. 4 ppm. These two peaks underlie the two main regions in the CP/MAS spectrum in Figure 5. In semicrystalline samples, interphase regions give more peaks between these values, further complicating the CP/MAS spectrum and changing peak intensities even more. Nonetheless, we are confident of the assignments of sharp peaks in the CP/MAS spectrum because of the extensive model compound evaluations we have carried out.

Room-temperature FT-IR analysis of copolymers **2a**, **2b**, and **3b** clearly indicates that the thioethylene segments are predominantly in gauche conformations in **2a** and **2b**. The CH_2 wagging mode was observed at 1186 cm^{-1} for **2a** and **2b** and at 1192 cm^{-1} for **3b**. In model compounds, this band moves to higher wavenumbers (from 1186 to 1196 cm^{-1}) as the length of the thioethylene segment decreases and the content of trans conformers increases.[17] The C−S stretching bands at 678 and 676 cm^{-1} for **2a** and **2b** are similar to that of PTE at 672 cm^{-1} and further confirm gauche conformations. This band was observed at 682 cm^{-1} for **3b**, consistent with a *trans*-thioether conformation. In fact, the FT-IR spectrum of cpolymer **3b** is very similar to that of the model compound with three sulfur atoms reported in the previous paper, which contained a 2:1 ratio of tt:tg conformations around the thioether units.

X-ray analysis was used to examine the differences in long range packing between the copolymers with oxyethylene and poly(methylene) units as spacers. Wide angle X-ray diffraction patterns (WAXD) of the copolymers **2a**, **2b**, and **3b** are given in Figure 6. Similar packing occurs in copolymers with oxyethylene spacer units (upper two traces), and the patterns observed for **2a** and **2b** correspond to that of PTE.[8] Copolymer **3b** showed an entirely different diffraction pattern, which was very similar to that of the model compound with three sulfur atoms in the backbone, indicating wider spacing between the polymer chains.[17] This would reduce the strength of the intermolecular interactions in the crystalline domains and is consistent with lower melting points for the copolymers with poly(methylene) segments than those with oxyethylene spacers.

Analysis of Thermal Behavior of $[(CH_2CH_2S)_n-CH_2CH_2O]_m$ polymers. Copolymer $[(CH_2CH_2S)_3-CH_2-CH_2O]_m$ (**2a**) has a melting point similar to that of a product obtained from the bis(isourea) intermediate (125−128 °C), indicating comparable structures and molecular weights.[10] This copolymer showed two endothermic transitions on repeated heating runs, but did not undergo any visible transformation at the first transition when observed under the optical microscope.

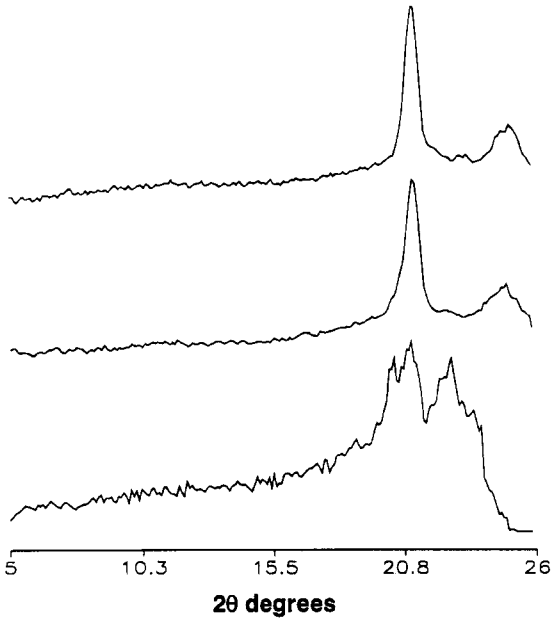

Figure 6. Wide angle X-ray diffraction patterns of solution-precipitated **2a**, **2b**, and **3b** (top to bottom).

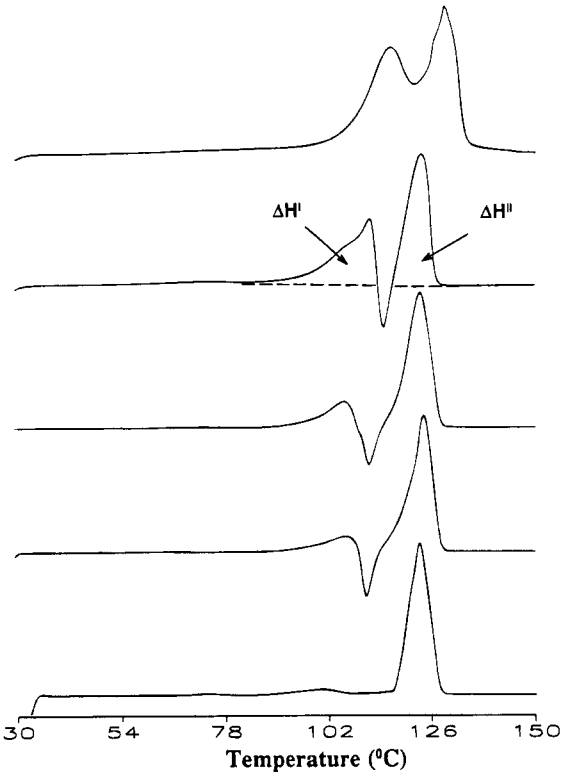

Figure 7. DSC traces of **2a** $[(CH_2CH_2S)_3-CH_2CH_2O]_m$ either after solution preparation, cooling from the melt at 2 °C/min, cooling at 20 °C/min, quenching from the melt with liquid N_2, or annealing at 118 °C (top to bottom).

This indicates that long range order in the solid state is maintained up to the actual melting transition. Figure 7 shows first-run DSC thermograms of copolymer **2a** samples that were either solution precipitated, cooled from the melt at 2 or 20 °C/min, quenched from the melt with liquid N_2, or annealed above the first transition (at 118 °C) for 2 h (top to bottom). Table 2 gives the transition temperatures and heat capacity (ΔH) values for these scans. A typical base line for the measurement of heat capacities from the DSC plot is shown on one of the traces.

The solution-precipitated sample had a heat capacity in the same range as those of the melt-crystallized

Table 2. DSC Data of Copolymer 2a $[(CH_2CH_2S)_3-CH_2CH_2O]_m$ after Different Thermal Histories[a] (See Also Figure 7)

sample history	T_c (°C)	ΔH_c (J/g)	T_m^I (°C)	T_m^{II} (°C)	ΔH^I (J/g)	ΔH^{II} (J/g)
solution precipitated			116.0	128.8	55.0	83.0
2.0[b]	107.0	96.0	111.0	124.8	37.0	80.0
20.0[b]	101.0	96.0	110.8	125.5	25.8	87.0
quenched[c]			109.6	126.0	16.4	87.5
annealed[d]			103.7	125.2	5.8	91.0

[a] T_c, crystalline temperature; ΔH_c, enthalpy of crystallization; T_m and ΔH, endotherm peak and corresponding enthalpy values for lower (I) and higher (II) transitions. [b] Cooling rates from the melt (°C/min). [c] Rapid cooling by immersion in liquid N_2. [d] Annealed for 2 h at 118 °C.

samples, but with a slightly higher transition temperature. In addition, no exotherm peak was observed between the two endotherms for this sample, perhaps because the two endotherms overlap and combine to completely compensate for the exotherm. For the melt-quenched samples, as the rate of cooling from the melt increased, the crystallization temperature was lowered but with no significant change in the enthalpy of crystallization (ΔH_c). In subsequent heating runs, two endotherms were observed with different intensities. Higher heat capacities for the initial endotherm (ΔH^I) were seen for samples that were cooled at 2 °C/min and solution precipitated (i.e., after slow crystallization). This thermal behavior is very similar to that seen for PBT and nylon 11, which show higher amounts of initial endotherms under slow cooling but higher amounts of the upper endotherms after rapid cooling.[16,23] The annealed sample showed virtually no evidence of either the lower endotherm or the intermediate exotherm and gave a melting enthalpy only slightly greater than those of the other samples. We interpret this to mean that the crystalline domains were locked into the form stable at higher temperature by annealing, and the sample therefore showed no melting of the crystal form stable at lower temperature because it was not present; therefore, no recrystallization into the higher temperature form occurred. Clearly, since the T_g's of both POE and PTE are well below room temperature, the sub-melting endotherm is associated not with amorphous regions but with the crystalline regions of the samples. If the molecular behavior associated with these transitions can be understood, it may be possible to control the crystallinity and, thus, the final thermal and physical properties of the copolymers through processing modifications.[26]

The absence of an observable physical transition under the microscope (polarized light with a hot stage) at the first DSC transition is consistent with a cooperative molecular transformation in crystalline domains, i.e., a crystal–crystal transition. Such behavior is also seen for PE, which exhibits a high-temperature hexagonal phase arising from a trans–gauche equilibrium developing below the melt, especially at high pressure.[24] Annealing in this high-temperature phase for PE causes crystal thickening and the formation of more extended chain crystals, which are observed during subsequent thermal analysis.[25,26] Under normal pressure, PE undergoes partial melting and recrystallization at these temperatures. The melting–recrystallization is so rapid for PE that only the highest temperature endothermic peak representing the recrystallized material normally is detected. Thus, the transition temperature observed does not represent the properties of the original crystallites.[27] It has been observed, however, that more perfect solution-formed crystals display resolved DSC

transitions for the initial crystallites, their recrystallization, and the subsequent melting of the high-temperature form.[28] Such a crystalline transformation is more likely to occur in the thioether copolymer than in PE due to the lower energy barrier between the different conformers at the C−S bonds (activation energy of 0.1 kcal/mol compared to 0.5 kcal/mol for C−C bond rotation). While cooperative motion thus might be presumed to lead to reorganization in the crystalline state, causing the intermediate exotherm, spectral evidence indicates otherwise.

Copolymer **2b** $[(CH_2CH_2S)_4-CH_2CH_2O]_m$ had a higher melting point than **2a** due to a higher thioether content. However, the difference (ca. 5 °C) is significantly smaller than the difference between $[(CH_2CH_2S)_2-CH_2CH_2O]_m$ and **2a** (ca. 60 °C). The lower ΔH values and melting temperatures for the precipitated and melt-crystallized samples of **2b** (compared to **2a**) suggest that a lower molecular weight polymer was obtained with the synthetic method used. Solution-precipitated **2b** had ΔH^{I} and ΔH^{II} values in the same range as those of the melt-crystallized samples, but with slightly higher transition temperatures. The thermal behavior of melt-crystallized **2b** is very similar to that of melt-crystallized **2a**, although the influence of the cooling rate was less significant. This might arise from more rapid crystallization due to the lower molecular weight (kinetically faster due to lower melt viscosity) and longer thioethylene segment than in **2a** (more stable crystals that form more rapidly).

If the multiple endotherms seen in varying quantities for samples with different thermal histories are related to widely different crystal forms, wide angle X-ray diffraction (WAXD) studies should detect differences in unit cell dimensions between a melt-crystallized sample (which has multiple endotherms) and an annealed sample (which has only the higher melting endotherm). Such differences in crystal packing have been established for poly(propylene) samples showing different DSC results.[29-31] Samples of **2a** and **2b** with the same thermal histories as those used for the thermal analyses described earlier were examined by WAXD. The patterns obtained (not shown) demonstrate that there is little apparent difference in overall crystal packing between the different samples. Thus, the submelting endotherm cannot be attributed to melting or large scale transformation of one type of crystal into another, but must be related to small changes occurring within the crystalline domains, and perhaps only within some of those. Like PE, the submelting transition in these thioether copolymers may involve only occasional gauche-to-trans jumps made possible by thermal expansion of the crystal lattice. X-ray and spectral data support this possibility.

The morphologies of samples of copolymer **2b** with different thermal histories were analyzed by SAXS (given in Figure 8). Both melt-quenched and solution-crystallized samples show a broad peak at ca. 60 Å. The peak shifts to lower 2θ (higher lamellar spacing) and merges with the quartz background peak after annealing at 110 °C for both samples. This confirms crystal thickening without apparent crystal form modification upon annealing (confirmed by WAXD patterns not shown), a process that must be related to significant mobility of the chain segments within the crystals.

Melt-crystallized **2b** was analyzed further by variable-temperature Raman, ^{13}C solid state NMR, and FT-IR techniques to further understand its molecular behavior. Figure 9 shows Raman spectra with increasing temperatures. At 50 °C, little change is observed in the gauche

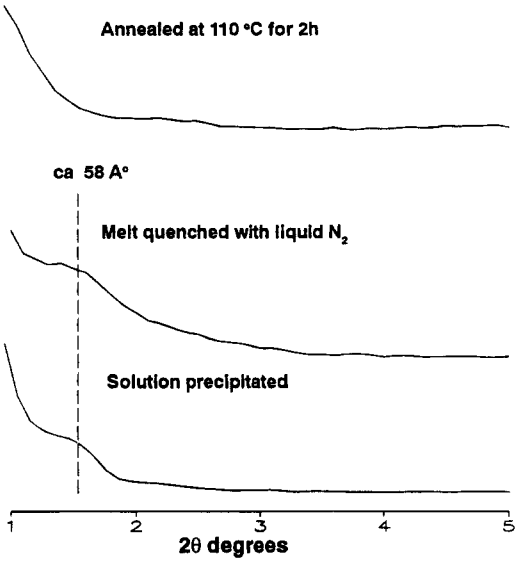

Figure 8. Small angle X-ray diffraction pattern of **2b** after different sample histories, as indicated.

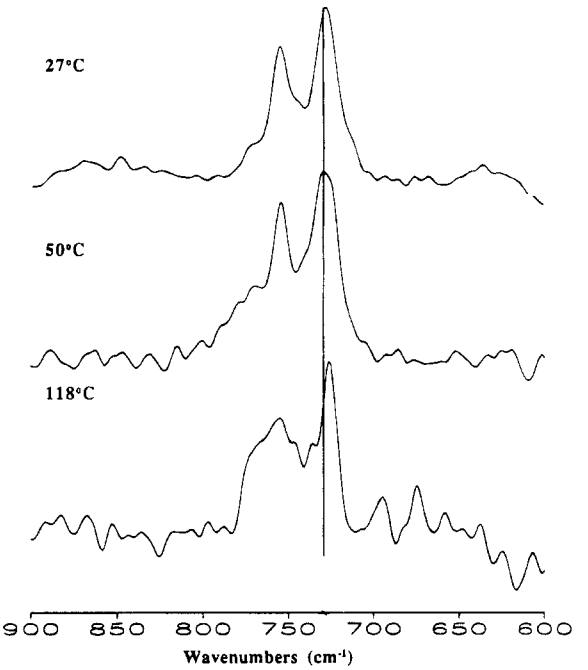

Figure 9. Variable-temperature Raman spectra of **2b** up to temperatures above the submelting transition but below T_m.

content, although there appears to be a broad peak beginning to grow at ca. 770 cm^{-1} corresponding to trans conformers. At 118 °C (above the first DSC-observed endotherm), the C−S asymmetric stretch for gauche units (753 cm^{-1}) shows broadening along with a significant increase in the trans isomer peak at 770 cm^{-1}. The C−S symmetric peak (vertical reference line at 727 cm^{-1}) possesses a shoulder in the 50 °C spectrum (at 720 cm^{-1}), which sharpens and becomes the predominant peak at 118 °C. Since the time scale of observation is very fast in Raman spectroscopy, even trans and gauche forms undergoing fast jump motions can be observed. Thus, in **2b** an increase in the C−S trans isomer content is observed without complete disappearance of the gauche peak, unlike the behavior of model compounds where complete gauche-to-trans isomerization was observed above the submelting transitions. High-temperature Raman analysis of PTE showed behavior similar to that of **2b**, with the gauche isomer peak at 756 cm^{-1} still present even at 180 °C, ca. only

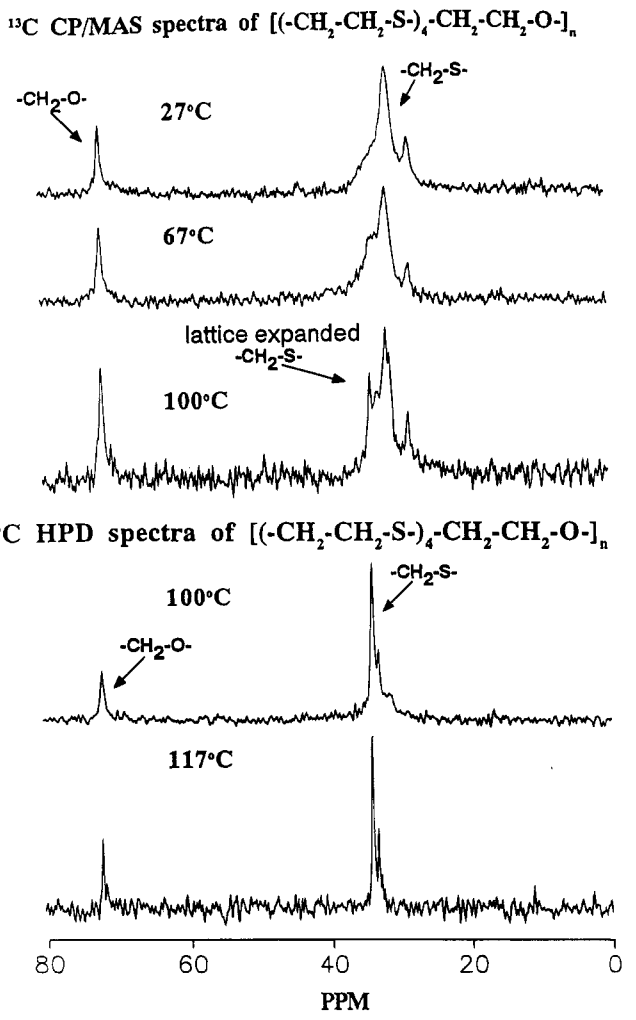

Figure 10. ^{13}C CP/MAS and HPD/MAS spectra of $[(CH_2CH_2S)_4-CH_2CH_2O]_m$ at the temperatures indicated.

20–30 °C below the melting point.[32] At this temperature, PTE has been reported to undergo crystal thickening (similar to the copolymers) as observed by longitudinal acoustic mode (low-frequency Raman) and SAXS analyses.[33,34] This behavior in both homo- and copolymers supports the coexistence of the gauche and trans conformers within the crystalline domains; i.e., thermal expansion of the crystal lattice allows occasional trans isomer formation that can propagate through the domain with rapid return to the more stable gauche isomer. As the sample temperature increases, the incidence or total number of such trans "defects" increases, as seen by increased trans peak intensity.

High-temperature ^{13}C CP/MAS and HP/MAS analyses were carried out on **2b**, and selected spectra are given in Figure 10. At room temperature there are peaks at 28.1 and 31.1 ppm (largest peak) for the methylene units β to oxygen and those between sulfur atoms (in their gg form), respectively, and at 71.6 ppm for methylene units α to oxygen. A broad peak is seen from 30 to 35 ppm for rigid amorphous domains; a broad peak at this same value for the mobile amorphous region is observed in the HP/MAS spectrum (not shown). By using this data with the Raman results, the preferred conformation at the C–S bonds is clearly found to be gauche (as drawn in Figure 4) at room temperature. When the sample is heated to 67 °C, the shoulder around 33 ppm increases, while the peaks at 31.1 and 28.1 ppm (now at 30.8 and 28.0 ppm) are somewhat reduced relative to the 71.6 ppm peak. The additional peak intensity at ca. 33 ppm cannot come from mobile amorphous regions because the sample temperature is well above the T_g and lack of cross-polarization for such mobile domains essentially eliminates their contribution. That is, because ^{13}C CP/MAS sees mainly rigid regions, the relative increase in this peak presumably comes from *crystalline* thioethylene segments undergoing jump motion between conformers and, therefore, experiencing less gauche shielding.

At 100 °C, the 33 ppm peak is resolved into two distinct peaks at 33.6 and 32.8 ppm. A temperature increase to 117 °C (spectrum not shown) causes these peaks (now at 33.9 and 32.9 ppm) to grow in intensity and the peaks (now) at 31.5 and 28.5 ppm to shrink further. Even above the DSC-observed transition (117 °C), molecular motion exists in only part of the crystalline regions because, first, peaks are observable (CP/MAS requires some rigidity) and, second, the peaks at 31.5 and 28.5 ppm are weak but still observable. Upon further heating to 127 °C, cross-polarization is lost because of sample melting. ^{13}C CP/MAS analysis thus confirms conformational disorder occurring *in* the crystalline domains at and above the submelting transition. This behavior is very different from that of the model compounds, which displayed *concerted* gauche-to-trans isomerization within the crystalline domains at the lower endothermic transition. However, it is also clear that molecular motion begins in the crystalline regions below the premelt transition, suggesting that nonconcerted libration develops gradually and continuously. Both observations are consistent with the less ordered crystalline regions of polymers; i.e., the crystalline domains are less perfect and domain sizes vary, both of which can result in "gradual" transitions, as observed on the macroscopic level or with analytical methods that "average" what is observed.

^{13}C HP/MAS spectra (Figure 10, lower spectra) at temperatures close to the submelting transition and up through the melt show three sharp peaks at 33.0, 33.9, and 71.9 ppm. These peaks are due to the methylene units in mobile amorphous regions (as confirmed by peak sharpness). The upfield peak at 33.9 ppm is also seen in the CP/MAS spectrum at 100 °C, indicating similar mobile gauche conformations near the surface or beginning to develop within the crystalline domains.

This molecular behavior observed upon heating **2b** is observed in reverse upon cooling the sample from the melt to below its crystallization temperature. Figure 11 gives various CP/MAS spectra upon cooling the sample analyzed in Figure 10. At temperatures down to 100 °C, cross-polarization is not possible due to high mobility; i.e., crystallization requires extended time and/or supercooling. At 90 °C, peaks appear at 34.0, 31.0, and 28.5 ppm, indicating that the sample initially crystallizes into the higher temperature form, with many of the crystalline thioethylene units completely gauche and some either held trans or exhibiting slow jump motion between the two conformers. This jump motion may be occurring in smaller crystallites or at the surface of larger ones.

Upon cooling down to 67 °C, peaks are still seen at 33.9 and 32.8 ppm, but with increased intensity for the peaks at 28.5 and 31.5 ppm, indicating the transformation of more trans-to-gauche conformations within crystalline domains. This spectrum looks very similar to the spectrum at 100 °C in the heating experiment, suggesting that the high-temperature phase formed upon heating requires some time to reform during the cooling cycle. This is confirmed by the additional changes observed in the 47 and 27 °C spectra. Despite the fact, then, that the sample shows a crystallization

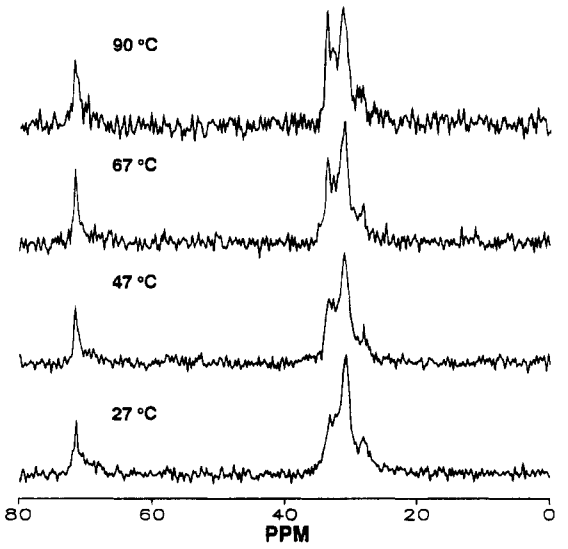

Figure 11. Variable-temperature ^{13}C CP/MAS spectra of $[(CH_2CH_2S)_4-CH_2CH_2O]_m$ upon cooling from the melt.

exotherm between 110 and 100 °C in the DSC, there is residual trans content present (in rigid domains) that only slowly rearranges to the gauche conformation at temperatures well below the crystallization temperature. Again, concerted molecular motion does not appear to be as strongly related to the DSC transitions observed as it is in the model compounds.

At room temperature, copolymer **2b** has IR bands at 2965 and 2929 cm^{-1}, corresponding to C−H asymmetric and symmetric stretches for the thioethylene segments. These bands coincide with the C−H asymmetric and symmetric stretches of PTE, indicating the presence of gauche conformations. There are weak bands corresponding to trans isomers at 2950 and 2914 cm^{-1}, which increase in intensity with temperature, while the bands at 2965 and 2929 cm^{-1} gradually decrease. Again, only gradual, apparently nonconcerted, changes are observed even upon going through the lower DSC endotherm. A similar trend is observed for cyclic model compounds containing 3−6 thioethylene units.[35] Conformational isomerism involving atoms with lone pairs of electrons has been evaluated for small molecules where it was recognized that a lone pair in a trans position weakens a C−H bond and reduces its vibrational frequency.[36] This effect is seen in **2b**, where increasing the trans isomer content at the C−S bond increases the low-frequency bands.

The integrated intensities of the C−H stretching peaks gave an additional indication of concerted processes for the model compounds, clearly indicating a discontinuity at the premelt.[19] Variation with temperature of the integrated area between 3050 and 2750 cm^{-1} for **2b** showed no discontinuous reduction, but rather showed two intersecting lines with a more rapid reduction in intensity above 100 °C. Complete melting at 130 °C, however, did cause a drastic reduction in the C−H stretching intensity. The FT-IR results support the NMR interpretation given here; i.e., no *concerted* gauche-to-trans isomerization occurs in this polymer, in contrast to the model compounds that clearly show *no* residual gauche content in the higher temperature crystal form. The conformational disorder observed in **2b** at intermediate temperatures does lead to crystal thickening (as observed by SAXS), a process that requires significant segmental motion but that occurs without the disruption of overall crystalline order and the mostly gauche conformations at the thioethylene units.

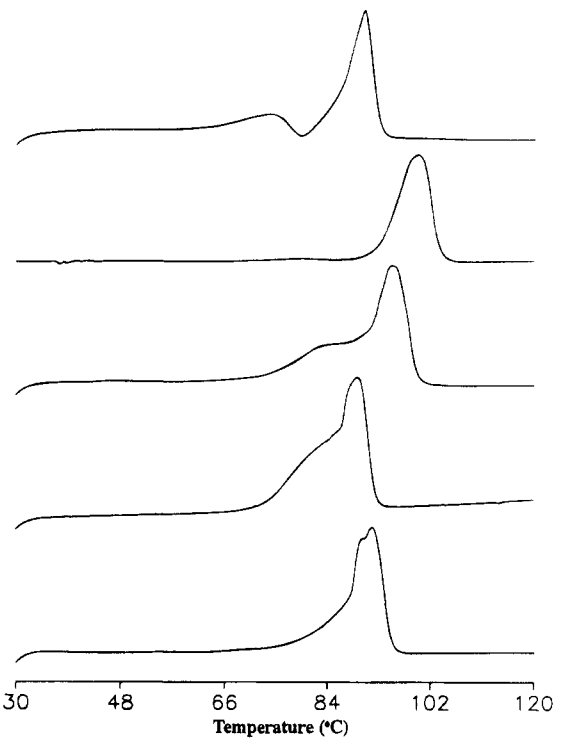

Figure 12. DSC heating traces of $[S(CH_2CH_2S)_2-(CH_2)_n]_m$ solution-precipitated samples, where n = 3, 5−8 (**3a**−**e**) from top to bottom.

Analysis of the Thermal Behavior of $[S(CH_2CH_2S)_2-(CH_2)_n]_m$. The first-run DSC thermograms of solution-precipitated samples of **3a**−**e** are given in Figure 12. Apparent melting points are all within 10 °C of each other, indicating that they are not influenced much by changing the length of the poly(methylene) segment, but are instead controlled by the crystalline packing of the thioethylene segments. Copolymers **3a**−**e** and **2a** have similar thioethylene segment lengths along the backbone, but the dissimilarity in their melting points indicates different crystalline packing; i.e., the oxyethylene spacer between the thioethylene units is more easily accommodated within the crystalline form preferred by the thioethylene segments than are the poly(methylene) spacers. We have observed that, in model systems, shorter lengths of thioethylene segments between decyl chains reduce the melting points to those of similar length linear alkanes due to the disruption of the preferred packing of the gauche thioether segments. That is, the intermolecular interactions between the thioethylene segments are reduced due to the alkyl chain forcing the terminal C−S bonds (of the thioether segments) to assume the less preferred trans conformation. A similar effect causes lower melting points in the copolymer series **3a**−**e** than in **2a** and **2b**.

The solution-precipitated sample of **3b** did not exhibit any submelting endotherm, although it and all *melt*-crystallized samples showed two endotherms with an overlapping exotherm. The ΔH values were not determined on all copolymer samples because of the proximity of the two endotherms (usually within 10 °C of each other, compared to >15 °C differences for **2a** and **2b**). Even annealing the samples above the submelting transition resulted in ΔH^{II} values that were significantly less than those of solution-precipitated samples. However, the values for various samples of **3b** (treated in the same manner as both **2a** and **2b**) were determined and are given in Table 3. In copolymers containing an oxyethylene spacer, ΔH^{II} values comparable to those of

Table 3. DSC Data of Copolymer 3b $[S(CH_2CH_2S)_2-(CH_2)_7]_m$ after Different Thermal Histories[a]

sample history	T_c (°C)	ΔH_c (J/g)	T_m^I (°C)	T_m^{II} (°C)	ΔH^I (J/g)	ΔH^{II} (J/g)
solution precipitated				104.0		76.5
2.0[b]	75.6	58.6	85.4	93.5	49.1	36.0
20.0[b]	64.7	62.2	85.0	94.0	37.6	42.8
quenched[c]			84.1	93.8	21.6	57.1
annealed[d]			79.2	95.8	7.6	44.6

[a] T_c, crystallization temperature; ΔH_c, enthalpy of crystallization; T_m and ΔH, endotherm peak and corresponding enthalpy values for lower (I) and higher (II) transitions. [b] Cooling rates from the melt (°C/min). [c] Rapid cooling by immersion in liquid N_2. [d] Annealed for 2 h at 85 °C.

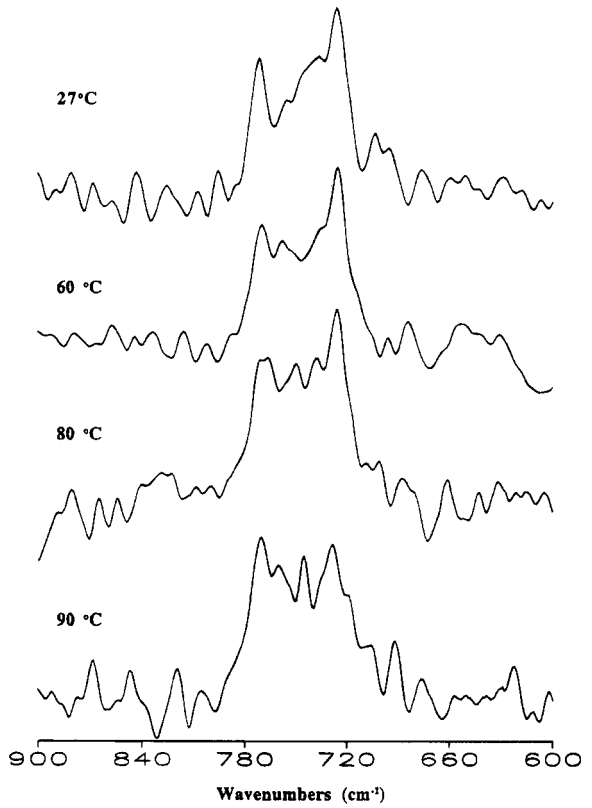

Figure 13. Variable-temperature Raman spectra of **3b** up to temperatures above the submelting transition.

solution-precipitated samples were obtained (Table 2), while this was not the case for **3b**. This may be related to reduced dipole interactions and increased molecular mobility at the thioethylene segments in **3a–e**, causing less efficient recrystallization than in **2a** and **2b**.

Because copolymer **3b** had the highest melting point and showed two distinct endotherms with an exotherm between when crystallized from the melt (not shown in Figure 12), it was chosen for more detailed thermal analysis with regard to the effect of sample history. Samples of copolymer **3b** with various sample histories gave similar WAXD traces and Raman and ^{13}C CP/MAS spectra when analyzed at ambient temperature. Differences in crystal perfection without changes in crystal form and amounts of crystallinity (similar to **2b**) therefore must be the cause of the differences in thermal behavior of **3b** samples. Moreover, SAXS analysis of copolymer **3b** showed no peak for lamellar spacing in either solution-precipitated or annealed samples.

Variable-temperature spectral analysis was applied to several samples of **3b**. Raman spectra at various temperatures are given in Figure 13. The strong peak at 770 cm^{-1} and weaker peak at ca. 750 cm^{-1} confirm

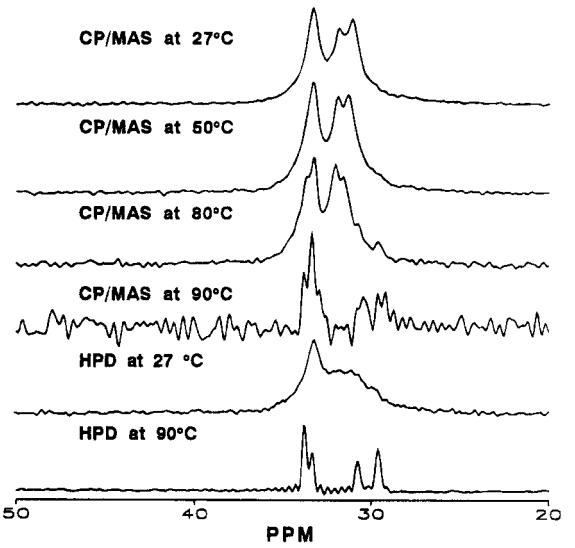

Figure 14. Selected ^{13}C CP/MAS and HPD/MAS spectra of **3b**.

the presence of both trans and gauche thioether conformations, with the former predominating in the ambient-temperature spectrum. Spectra at increasing temperatures clearly show a relative increase in the former and multiplicity with (perhaps) reduction in the latter. Even above the first transition temperature (ca. 85 °C), it is not clear from these spectra that all of the gauche peak has disappeared. Thus, while the onset of conformational motion at the C–S bonds begins at ca. 50 °C, no clearly concerted process was observed at the lower transition. High-temperature FT-IR analysis of **3b** also did not clearly show shifts in bands, but did show a different rate of reduction in the C–H stretching intensity above 85 °C, the temperature corresponding to the initial endotherm. Upon going through the melt, however, the sample (observed at 100 °C) did show a discontinuous drop in integrated intensity.

High-temperature ^{13}C CP/MAS and HP/MAS analyses were carried out on **3b** up through the initial DSC endotherm, i.e., to 90 °C (Figure 14). At 50 °C, there is reduction in the peak at 31.3 ppm along with a shift to 31.5 ppm; the *all-trans*-poly(methylene) segment peak at 33 ppm is unchanged. This behavior is similar to what is observed in the model compounds, confirming an initial gauche-to-trans libration or an isomerization process for some of the thioethylene segments in crystalline domains of **3b**. At the same time, the peak at 31.9 ppm shifts to 32.1 ppm and increases in intensity relative to the 31.5 and 33 ppm peak. At 80 °C, the peaks at 32.1 and 31.5 ppm both move downfield by ca. 0.2 ppm and two new peaks appear, one as a shoulder at 31.0 ppm and the other at 29.0 ppm, both caused by γ-gauche interactions within the poly(methylene) units. A new shoulder is also seen on the 33 ppm peak (ca. 33.4 ppm), which corresponds to the peak in the 90 °C spectrum due to mobile thioethylene carbons. The spectrum obtained just above the DSC transition (90 °C) is very different from the others. First, CP/MAS observation indicates that cross-polarization is still possible, and the domains seen are still relatively rigid. However, the two sets of peaks seen at around 33.0 and 30.0 ppm now result from the complete disappearance of gauche thioether units and *trans*-poly(methylene) segments. The first set of peaks (at ca. 33.0 ppm) corresponds to the methylene units adjacent to sulfur involved in jump motions between trans and gauche conformers, causing a shift to higher ppm values similar to what was observed for **2b**. The second set arises from

the carbons of the poly(methylene) spacer in a conformationally disordered state experiencing rotationally averaged trans–gauche interactions. The multiplicity of both sets of peaks arises from different chemical environments (composition of attached groups) plus gauche–trans isomerization within the increasingly disordered crystalline domains.

The ^{13}C HP/MAS spectrum at 90 °C shows liquid-like conformationally averaged peaks at 33.8, 33.4, 30.8, and 29.6 ppm, which correspond to the peaks seen in the CP/MAS spectrum at the same temperature. The relative intensities of these peaks correspond to 4:2:2:3, as expected for this copolymer structure. In contrast to copolymer **2b**, where some gauche conformations are maintained above the submelting transition, in **3b** the disorder develops more extensively through the sample and within the residual crystalline regions. This copolymer, perhaps because it is more like the model compounds in overall composition and is less tightly packed in its crystalline domains than **2a** and **2b**, appears to display a more concerted crystal–crystal transformation. Examination of the DSCs and spectra of the other poly(methylene) copolymers in this series indicates that they display similar behavior.

Conclusions. Room-temperature spectroscopic analysis of the copolymers confirmed conformations similar to that of PTE around the thioethylene segments in those with oxyethylene spacers, i.e., mostly gauche isomers. Those with poly(methylene) spacers, however, displayed conformational behavior more like that of the shorter oligo(thioethylene) model compounds reported in the previous paper (mostly trans conformations at the C–S bonds). This reduces the intermolecular interactions between the polymer chains in the latter and results in an entirely different type of crystal packing (as seen by WAXD and lower melting points) and molecular behavior at the lower DSC endothermic transition (concerted rather than nonconcerted gauche-to-trans isomerization). It is clear from a comparison of the results obtained from the model compounds with those from the copolymers that the models offer easier to interpret spectral information that correlates more readily with thermal transitions. Polymers are more complicated and less well behaved for a number of reasons, including molecular weight distributions, variations in crystal size and perfection, the presence of interlamellar polymer chains, and the occurrence of adjacent versus nonadjacent reentry of chains into crystal lattices. The observation of first-order premelt transitions in the DSC may (probably does) indicate concerted crystal–crystal transformation of some crystals or some regions of a given crystalline domain in the polymers, but the overall imperfections certainly can account for both the fact that the onset of motion within the crystalline domains appears to occur significantly below the premelt transition and the fact that a significant portion of the crystalline regions does not undergo concerted transformation at the premelt (at least for the oxyethylene-containing copolymers). Nonetheless, the detailed and extensive spectral analyses summarized in these two papers clearly confirm the presence of the preferred gauche conformations around thioethylene oligomer segments in model compounds and copolymers and confirm that there is significant gauche-to-trans isomerization of these groups below, but especially above, the premelt transitions observed for virtually all of the materials examined here. This work also points out the need for careful synthetic and spectral exploration of the given family of polymers and model compounds of interest. More importantly, it is clear from this work that the use of one or two spectral methods rarely supplies the range of information needed to extensively or completely understand polymer behavior, especially when attempting to correlate molecular and macroscopic properties.

Acknowledgment. This work was supported in part by Enimont Chemical Co. We acknowledge Dr. W. L. Jarrett and Dr. C. G. Johnson for acquiring the solid state NMR spectra.

References and Notes

(1) Price, C.; Evans, K. A.; Booth, C. *Polymer* **1975**, *16*, 6468.
(2) Brandrup, J.; Immergut, E. H. *Polymer Handbook*; Interscience: New York, 1989.
(3) Abe, A. *Macromolecules* **1980**, *13*, 546.
(4) Abe, A. *Polym. Prepr., Am. Chem. Soc. Div. Polym. Chem.* **1979**, *20* (1), 460.
(5) de Chirico, A.; Zotteri, L. *Eur. Polym. J.* **1975**, *11*, 487.
(6) Dalley, N. K.; Larson, S. B.; Smith, J. S.; Matheson, K. L.; Izatt, R. M.; Christensen, J. J. *J. Heterocycl. Chem.* **1981**, *18*, 463.
(7) Murray, S. G.; Hartley, F. R. *Chem. Rev.* **1981**, *81*, 365.
(8) Takahashi, Y.; Tadokoro, H.; Chatani, Y. *J. Macromol. Sci.—Phys.* **1968**, *B2*, 361.
(9) Mathias, L. J.; Canterberry, J. B. *Macromolecules* **1980**, *13*, 1723.
(10) Mathias, L. J.; Canterberry, J. B. *Crown Ethers and Phase Transfer Catalysis in Polymer Science*; Mathias, L. J., Carraher, C. E., Jr., Eds.; Plenum Press: New York, 1984; p 359.
(11) Sianawati, E.; Van De Mark, M. R. *Polym. Mater.: Sci. Eng.* **1989**, *61*, 709.
(12) Sianawati, E.; Van De Mark, M. R. *J. Polym. Sci., Polym. Chem.* **1992**, *24*, 119.
(13) Angiolini, L.; Carlini, C.; Tramontini, M.; Ghedini, N. *Polymer* **1990**, *31*, 353.
(14) Yeh, J. T.; Runt, J. *J. Polym. Sci., Polym. Phys.* **1989**, *27*, 1543.
(15) Xenopoulos, A.; Wunderlich, B. *J. Appl. Polym. Sci.* **1990**, *28*, 2271.
(16) Mathias, L. J.; Powell, D. G.; Austran, J. P.; Porter, R. S. *Macromolecules* **1990**, *23*, 963.
(17) Muthiah, J.; Johnson, C. G.; Thompson, R. T.; Mathias, L. J. *Macromolecules* **1995**, *28*, 7796.
(18) Shaffer, T. D.; Kramer, M. C. *Makromol. Chem.* **1990**, *191*, 71.
(19) Zhang, T.; Litt, M. H.; Rogers, C. E. *J. Polym. Sci., Polym. Chem.* **1994**, *32*, 1323.
(20) Watanabe, J.; Krigbaum, W. R. *Macromolecules* **1984**, *17*, 2288.
(21) Riande, E.; Guzman, J. *Macromolecules* **1979**, *12*, 952.
(22) Kurosu, H.; Ando, I. *J. Mol. Spectrosc.* **1990**, *239*, 149.
(23) Hobbs, S. Y.; Pratt, C. F. *Polymer* **1975**, *16*, 462.
(24) Wunderlich, B.; Grebowicz, J. *Adv. Polym. Sci.* **1984**, *60/61*, 1.
(25) Wunderlich, B.; Arakawa, T. *J. Polym. Sci. Part A* **1964**, *2*, 3697.
(26) Wunderlich, B.; Melillo, L. *Makromol. Chem.* **1968**, *118*, 250.
(27) Alamo, R.; Mandelkern, L. *J. Polym. Sci. Polym. Phys. Ed.* **1986**, *24*, 2087.
(28) Mandelkern, L.; Allou, A. L. *J. Polym. Sci. B* **1966**, *4*, 447.
(29) Pae, K. D. *J. Polym. Sci.* **1968**, *A-26*, 657.
(30) Jones, A. T.; Aizelwood, J. M.; Beckett, D. R. *Makromol. Chem.* **1964**, *75*, 134.
(31) Forgacs, P.; Tolochko, B. P.; Sheromov, M. A. *Polym. Bull.* **1981**, *6*, 127.
(32) Mathias, L. J.; Muthiah, J. Unpublished results.
(33) Hendra, P. J.; Majid, H. A. *J. Mater. Sci.* **1975**, *10*, 1871.
(34) Noether, H. D. *J. Mater. Sci.* **1976**, *11*, 1971.
(35) Mathias, L. J.; Muthiah, J. *Polym. Prepr.* **1990**, *31* (2), 649.
(36) McKean, D. C. *Chem. Soc. Rev.* **1978**, *7*, 399.

MA9502718